Cellular/Molecular

The Neuronal Serum- and Glucocorticoid-Regulated Kinase 1.1 Reduces Neuronal Excitability and Protects against Seizures through Upregulation of the M-Current

Pablo Miranda,[1,2] Alba Cadaveira-Mosquera,[4] Rafaela González-Montelongo,[1,2] Alvaro Villarroel,[5] Tomás González-Hernández,[2] J. Antonio Lamas,[4] Diego Alvarez de la Rosa,[2] and Teresa Giraldez[1]

[1]Research Unit, University Hospital NS Candelaria, 38010 Santa Cruz de Tenerife, Spain, Departments of [2]Physiology and [3]Anatomy and Institute of Biomedical Technologies, University of La Laguna, 38071 La Laguna, Spain, [4]Department of Functional Biology, University of Vigo, 36310 Vigo, Spain, and [5]Biophysics Unit, Spanish National Research Council–University of the Basque Country, 48940 Leioa, Spain

The M-current formed by tetramerization of Kv7.2 and Kv7.3 subunits is a neuronal voltage-gated K^+ conductance that controls resting membrane potential and cell excitability. In *Xenopus laevis* oocytes, an increase in Kv7.2/3 function by the serum- and glucocorticoid-regulated kinase 1 (SGK1) has been reported previously (Schuetz et al., 2008). We now show that the neuronal isoform of this kinase (SGK1.1), with distinct subcellular localization and modulation, upregulates the Kv7.2/3 current in *Xenopus* oocytes and mammalian human embryonic kidney HEK293 cells. In contrast to the ubiquitously expressed SGK1, the neuronal isoform SGK1.1 interacts with phosphoinositide-phosphatidylinositol 4,5-bisphosphate (PIP_2) and is distinctly localized to the plasma membrane (Arteaga et al., 2008). An SGK1.1 mutant with disrupted PIP_2 binding sites produced no effect on Kv7.2/3 current amplitude. SGK1.1 failed to modify the voltage dependence of activation and did not change activation or deactivation kinetics of Kv7.2/3 channels. These results suggest that the kinase increases channel membrane abundance, which was confirmed with flow cytometry assays. To evaluate the effect of the kinase in neuronal excitability, we generated a transgenic mouse (Tg.sgk) expressing a constitutively active form of SGK1.1 (S515D). Superior cervical ganglion (SCG) neurons isolated from Tg.sgk mice showed a significant increase in M-current levels, paralleled by reduced excitability and more negative resting potentials. SGK1.1 effect on M-current in Tg.sgk–SCG neurons was counteracted by muscarinic receptor activation. Transgenic mice with increased SGK1.1 activity also showed diminished sensitivity to kainic acid-induced seizures. Altogether, our results unveil a novel role of SGK1.1 as a physiological regulator of the M-current and neuronal excitability.

Introduction

The M-current is a voltage-dependent non-inactivating potassium conductance found in many neuronal types (Brown and Adams, 1980; Marrion, 1997). This current, generated by members of the Kv7 channels family, activates at voltages in the range of neuronal action-potential initiation, playing a central role in neuronal excitability and firing frequency modulation (Wang et al., 1998; Gutman et al., 2003; Tzingounis and Nicoll, 2008). In many brain regions, M-currents are mediated by Kv7.2/Kv7.3 heteromers. Mutations in their encoding genes, KCNQ2 or KCNQ3, cause a form of juvenile epilepsy called benign familial neonatal convulsions (Biervert et al., 1998; Charlier et al., 1998; Schroeder et al., 1998; Singh et al., 1998). The muscarinic pathway inhibits the Kv7.2/3 current (Brown and Adams, 1980; Marrion et al., 1989) through regulation of phosphoinositide-phosphatidylinositol 4,5-bisphosphate (PIP_2) levels, a phospholipid that activates the channel by direct binding (Suh and Hille, 2002; Zhang et al., 2003; Li et al., 2005; Winks et al., 2005; Falkenburger et al., 2010a). Other receptors and messengers regulate the M-current (Marrion, 1997; Hernandez et al., 2008), leading to a model in which PIP_2, calcium–calmodulin, and protein kinase C interplay to regulate Kv7 function (Delmas and Brown, 2005; Kosenko et al., 2012).

The Src–tyrosine kinase (Gamper et al., 2003; Li et al., 2004) and the serum- and glucocorticoid-regulated kinase 1 (SGK1; Schuetz et al., 2008) have also been proposed to regulate M-current. SGK1 is a ubiquitously expressed serine–threonine kinase playing an important physiological role in kidney, in which it regulates the epithelial sodium channel (ENaC) function, mainly by enhancing steady-state channel plasma membrane abundance (Alvarez de la Rosa et al., 1999). SGK1

Received July 18, 2012; revised Nov. 8, 2012; accepted Dec. 7, 2012.

Author contributions: P.M., A.V., J.A.L., D.A.d.l.R., and T.G. designed research; P.M., A.C.-M., R.G.-M., T.G.-H., D.A.d.L.R., and T.G. performed research; P.M., A.C.-M., R.G.-M., T.G.-H., J.A.L., D.A.d.l.R., and T.G. analyzed data; A.V., T.G.-H., J.A.L., D.A.d.l.R., and T.G. wrote the paper.

This work was funded by the Institute of Salud Carlos III/Directorate General for Evaluation and Research Promotion Grants PI09/00406 and PI12/00428 and Spanish Ministry of Science and Innovation Grants Consolider-Ingenio CSD2008-000005, BFU2010-16615/BFI, and BFU2008-02952/BFI and was cofinanced by the European Regional Development Funds "A Way of Making Europe" from the European Union. T.G. is supported by Programa Miguel Servet (Institute of Salud Carlos III/Directorate General for Evaluation and Research Promotion). We thank Andrew J. Plested, Patricio Rojas, and George K. Chandy for comments on this manuscript, Cecilia M. Canessa for providing us with the Nedd4-2 and SGK1.1 plasmids, Jonathan Barroso-González for helpful recommendations on the flow cytometry experiments, Carlos Flores and Almudena Corrales for advice and help using PCR mRNA prolifer arrays, and M. Rosa Arnau for excellent animal care.

The authors declare no competing financial interests.

Correspondence should be addressed to T. Giraldez, Research Unit, University Hospital NS Candelaria, 38010 Santa Cruz de Tenerife, Spain. E-mail: giraldez@ull.es.

DOI:10.1523/JNEUROSCI.3442-12.2013

 0270-6474/13/332684-13$15.00/0

phosphorylates the ubiquitin-ligase Nedd4-2, disrupting its interaction with ENaC through a C-terminal PPxY (PY) motif and leading to channel reduced endocytosis levels (Staub et al., 1996; Debonneville et al., 2001; Kamynina et al., 2001; Snyder et al., 2002). Other ion channels regulated by the SGK1/Nedd4-2 pathway include CLC2 (Palmada et al., 2004) and Kv1.3 (Henke et al., 2004). SGK1.1, a neuronal splice isoform of SGK1, has been characterized recently with two distinctive features: (1) SGK1.1 is highly expressed in the nervous system, in which it regulates ion channels, including the acid-sensing ion channel 1 (ASIC1) and δ-ENaC (Arteaga et al., 2008; Wesch et al., 2010); (2) it presents distinct plasma membrane localization, through PIP_2 binding to a N-terminal polybasic–amino acid cluster (Arteaga et al., 2008; Raikwar et al., 2008).

In this work, we hypothesized that the neuronal SGK1.1 is a physiological M-current regulator. In heterologous expression systems, it induces an increase in Kv7.2/3 current levels as a result of enhanced channel plasma membrane abundance, involving a PY-motif-independent, Nedd4-2-mediated mechanism. Superior cervical ganglion (SCG) sympathetic neurons isolated from transgenic (Tg) mice with boosted SGK1.1 activity show enhanced M-current levels, an effect that can be totally abrogated by muscarinic receptor activation. Accordingly, Tg SCG neurons showed reduced cell excitability and more negative resting membrane potentials. Tg mice were resistant to kainic acid (KA)-induced seizures, showing that SGK1.1 can regulate neuronal excitability through M-current modulation.

Materials and Methods

Animal handling and all experimental procedures were approved by the Spanish Higher Research Council, the University of La Laguna, and the University of Vigo Scientific Committee, and they conformed to Spanish and European guidelines for the protection of experimental animals (RD1201/2005; 2010/63/EU).

DNA cloning, mutagenesis, and cRNA synthesis

Human Kv7.2 (Y15065) and Kv7.3 (NM004519) cDNAs were provided by T. Jentsch (Leibniz Institute for Molecular Pharmacology, Berlin, Germany) and subcloned into pSRC5. Point mutation A315T of Kv7.3 was introduced by PCR (Etxeberria et al., 2004). For flow cytometry assays, Kv7.2 and Kv7.3 subunits were tagged with a tandem repeat of two hemagglutinin (HA) epitopes (YPYDVPDYA) and then subcloned into pcDNA3.1 (Invitrogen) (Gómez-Posada et al., 2011). Mouse SGK1.1 and Nedd4-2 cloned in pcDNA3.1/V5–His–TOPO (Invitrogen) were kind gifts from Dr. Cecilia M. Canessa (Yale University, New Haven, CT). KKR- and K220A–SGK1.1 mutants were generated as described previously (Wesch et al., 2010). The constructs were used as templates for *in vitro* transcription with the mMessage mMachine cRNA synthesis kit (Ambion) or used directly for transfection.

Mouse transgenesis

A bacterial artificial chromosome (BAC) containing 180 kb of mouse genomic DNA that includes the full SGK1 gene but no other known or predicted genes was obtained from the BACPAC Resources Center (Children's Hospital Oakland Research Institute, Oakland, CA). The BAC was modified by homologous recombination in *Escherichia coli* (Lalioti and Heath, 2001) to add three copies of the HA epitope in the COOH terminus of SGK1 and a point mutation (S422D in SGK1, S515D in SGK1.1) that renders the kinase constitutively active (Kobayashi and Cohen, 1999; Arteaga et al., 2008). The integrity of the modified BAC was tested by sequencing the extremes of the insert and by Southern blotting. The BAC insert was excised by digestion with NotI, purified by field inversion gel electrophoresis, followed by digestion with β-agarase and used for pronuclear injection of (C57BL/6J × SJL/J) F2 embryos. Genotyping was performed by PCR analysis of genomic DNA using primers 5′- GGAA GCAGCAGAAGCCTTCCTCGG-3′ and 5′- GACTGCCAAGCTTCCA GGTGTGC-3′, which flank SGK1 stop codon and produce a 186 bp product with wild-type SGK1 and a 267 bp product with Tg.sgk attributable to the insertion of three consecutive copies of the HA epitope. Founder animals harboring the transgene were crossed with C57BL/6 mice. Mice homozygous for the transgene were obtained by crossing heterozygous animals.

Analysis of gene expression

SCGs from control or Tg mice ($n = 7$) were dissected and pooled in RNAlater (Qiagen) to preserve tissue RNA. Total RNA was obtained from tissues disrupted with a Tissue Tearor (BioSpec Products) using a commercial kit (Illustra RNAspin mini kit; GE Healthcare) following the protocol of the manufacturer, which includes in-column DNase digestion to avoid contamination by genomic DNA. Purified total RNA was quantified using a Nanodrop. Equal amounts of total RNA were processed with the iScript cDNA synthesis kit (Bio-Rad) using oligo-dT as primer.

Endogenous and Tg SGK1 were simultaneously detected by RT-PCR using primers 5′-GGAAGCAGCAGAAGCCTTCCTCGG-3′ and 5′-GA CTGCCAAGCTTCCAGGTGTGC-3′. Templates obtained from cDNA synthesis reactions without reverse transcriptase were used to ensure the absence of genomic DNA contamination. RT-PCR products were analyzed in a 2% agarose gel and stained with ethidium bromide.

Quantitative PCR (qPCR) was performed using cDNA as template and the following oligonucleotide pairs (5′ to 3′): forward SGK1, CGGTTT CACTGCTCCCCTCAGTC;reverseSGK1,GCGATGAGAATCGCTACC ATTCCC; forward, SGK1.1, GAAGGCGGATCGGGATACAGATGC; and reverse SGK1.1, CTTTGGAAAGCATGGTCACCCAG.

Each qPCR reaction was performed in triplicate using the iQ SYBR Green Supermix (Bio-Rad) in a Mini Opticon real-time PCR machine (Bio-Rad). Threshold cycle (Ct) analysis was performed with the software of the manufacturer. Primer pairs were evaluated for their efficiency using serial dilutions of cDNA. Relative quantification of mRNA abundance was performed by comparison with a GAPDH amplicon using the comparative Ct method (Schmittgen and Livak, 2008). Data are expressed as average ± SD. The specificity of the qPCR reaction was assessed by melting-temperature analysis and agarose gel electrophoresis of the end-point products.

To profile the expression of 84 ion channels and transporters involved in neuronal function in control or Tg.SGK1 SCGs, we used a commercial low-density qPCR array (RT^2 Prolifer PCR Array; Qiagen). One microgram of total SCG RNA prepared as described above was used to generate cDNA with the RT^2 first-strand kit (Qiagen). qPCR reactions were performed in 96-well plates already containing oligonucleotide pairs using RT^2 SYBR Green master mix (Qiagen) in a real-time cycler (Applied Biosystems 7500 Fast). The array included five housekeeping genes, a control for contamination with genomic DNA, three controls for the efficiency of cDNA synthesis, and three positive PCR controls. Melting-temperature analysis and Ct calculation was performed using the software of the manufacturer. Ct values were exported and analyzed using an Excel spreadsheet provided by the array manufacturer (Qiagen). We analyzed the 84 genes included in the kit, but nine of them gave unreliable results so the final output was of 75 genes tested.

Cell culture

Heterologous expression in human embryonic kidney 293 cells. Human embryonic kidney 293 (HEK293) cells (American Type Culture Collection) were maintained in DMEM (Invitrogen) supplemented with 100 UI/ml penicillin, 1.1 mg/ml streptomycin, and 10% FBS (Sigma), at 37°C. Cells were split and plated at 40% density on sterile poly-L-lysine (0.01%; Sigma)-coated coverslips and transiently transfected after 24 h (Wesch et al., 2010; Gómez-Posada et al., 2011). The transfection mixture included 2 μl of Lipofectamine 2000 (Invitrogen) and DNA with the following combinations: Kv7.2/3, 200 ng of each; Kv7.2, 400 ng; Kv7.3–A315T or Kv7.3, 400 ng; Kv7.2/3 (200 ng/each) with SGK1.1, KKR, or K22A mutants (100 ng); Kv7.2/3 (200 ng/each) with SGK1.1 (100 ng) with or without Nedd4-2 (100 ng). For flow cytometry assays, DNA quantities were increased to Kv7.2–HA (1 μg) with Kv7.3–HA (1 μg) with or without SGK1.1 (1 μg). Cells were incubated for another 24–48 h before performing electrophysiological recordings or flow cytometry assays.

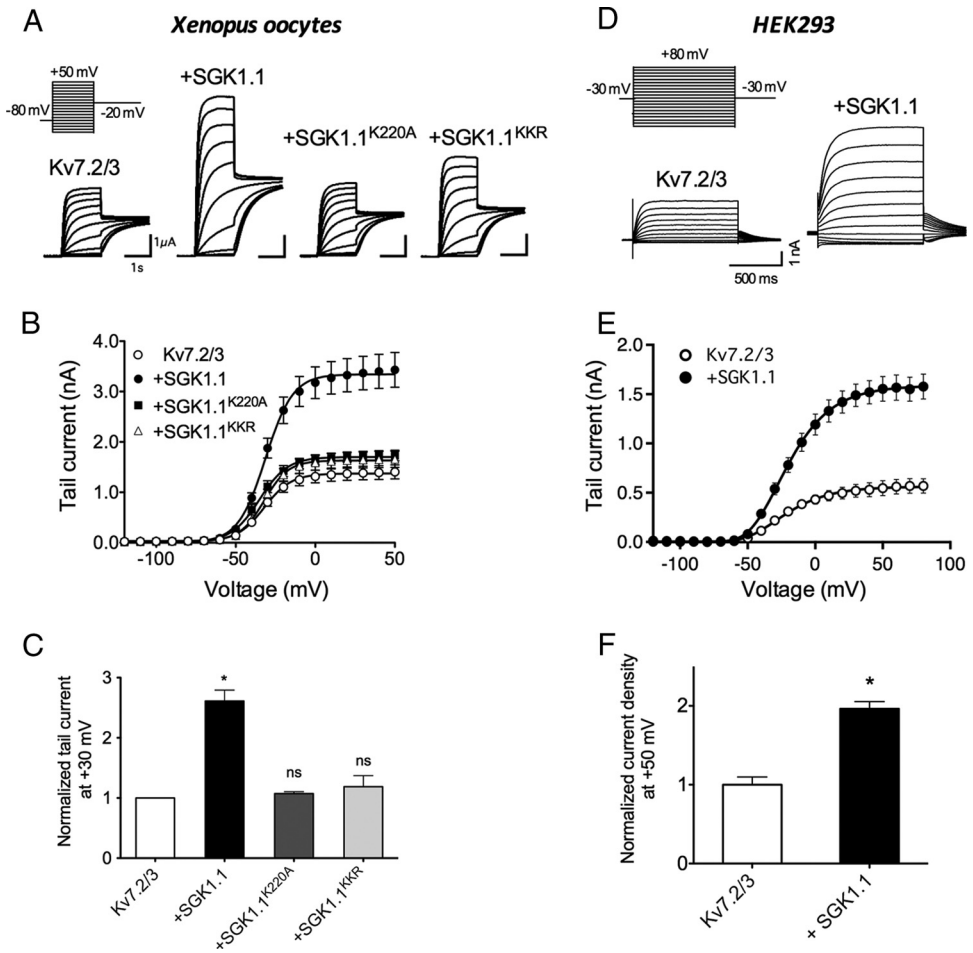

Figure 1. SGK1.1 increases Kv7.2/3 currents. ***A***, Currents elicited in *Xenopus* oocytes after coinjection of mRNAs from Kv7.2/3 channels alone (first panel) or in combination with wild-type SGK1.1 (second panel), mutant SGK1.1–K21N/K22N/R23G (SGK1.1^{KKR}; third panel), or SGK1.1–K220A (SGK1.1^{K220A}; fourth panel). Oocytes were maintained at a holding potential of −80 mV, and sequential depolarizing pulses ranging from −120 to +50 mV were applied, followed by a −20 mV pulse (inset). For clarity, only representative traces corresponding to −70 to +30 mV depolarizing pulses are shown. ***B***, Average activation curves and corresponding fits to Boltzmann equations (solid lines) for the construct combinations indicated in the graph legend ($n \geq 20$, $n =$ 5 oocyte batches). ***C***, Tail currents measured at −20 mV after +30 mV depolarizing pulses for the indicated construct combinations. Values were normalized to Kv7.2/3 tail currents ($n \geq 20$, $n =$ 5 batches). *$p < 0.05$; ns, not significant. ***D***, Representative current families elicited in HEK293 cells transfected with Kv7.2 and Kv7.3 DNA with or without SGK1.1, corresponding to a protocol of depolarizing pulses ranging from −120 to +80 mV in 10 mV steps and a repolarization step to −30 mV. For clarity, only pulses from −70 to +50 mV are shown. ***E***, Average activation curves and corresponding fits to Boltzmann equations for the construct combinations indicated in the graph legend ($n \geq 11$). ***F***, Normalized tail current density values measured after +50 mV depolarizing pulses for the indicated construct combinations. Values were normalized to Kv7.2/3 tail currents. *$p < 0.05$.

SCG cell culture. Neurons from the mouse SCG were cultured as described previously (Romero et al., 2004; Lamas et al., 2009). In brief, 20- to 60-d-old mice were terminally anesthetized with CO_2 and decapitated. Ganglia were removed under a binocular microscope and washed in L-15 Leibowitz medium. After being split, the ganglia were incubated in collagenase (2.5 mg/ml in HBSS) for 15 min and in trypsin (1 mg/ml in HBSS) for 30 min at 37°C. After the enzymatic treatment, neurons were mechanically isolated, centrifuged, and plated in 35 mm Petri dishes previously coated with laminin (10 μg/ml in EBSS). Neurons were recorded after 1–2 d in culture, and only round-shaped neurons basically devoid of processes were used (Romero et al., 2004). Culture medium (kept at 37°C and 5% CO_2) was L-15 containing 24 mM $NaHCO_3$, 10% FBS, 2 mM L-glutamine, 38 mM D-glucose, 100 UI/ml penicillin, 100 μg/ml streptomycin, and 50 ng/ml nerve growth factor.

Heterologous expression of Kv7.2/3 in Xenopus *oocytes*

Adult females Xenopus were anesthetized by immersion in tap water containing 1.7 g/L tricaine. Oocytes were harvested by partial ovariectomy and collagenase dispersion (Barros et al., 1998). Stage V–VI oocytes were selected and microinjected with 5–10 ng of cRNA. After injection, oocytes were incubated for 1–2 d at 17°C in oocyte Ringer's solution (OR-2) containing the following (in mM): 82.5 NaCl, 2 KCl, 2 $CaCl_2$, 2 $MgCl_2$, 2 Na_2HPO_4, and 10 HEPES, pH 7.4.

Electrophysiology

Two-electrode voltage clamp in Xenopus *oocytes.* Whole-cell currents were recorded as described previously (Wesch et al., 2012) using two-electrode voltage clamp with an OC-725C amplifier (Warner Instruments). Oocytes were perfused with OR-2 (in mM: 82.5 NaCl, 2.5 KCl, 1 $MgCl_2$, 2.5 $CaCl_2$, and 5 HEPES, pH 7.4) and clamped at a holding potential of −80 mV. Activation curves were generated by increasing the voltage from −120 to +50 mV in 10 mV steps of 1.5 s, followed by a −20 mV pulse of 2 s, in which tail currents were measured. Deactivation was studied by applying a depolarization pulse to +50 mV to maximize channel aperture, followed by repolarizing pulses to voltages ranging from −30 to −120 mV, in which the decay phase of the current was analyzed. Non-injected oocytes showed no endogenous M-currents or any other endogenous current in response to voltage protocols used.

Perforated patch-clamp experiments on HEK293 cells. Ionic current recordings in HEK293 cells were performed at room temperature (~23°C) in the perforated patch configuration of the patch-clamp technique as described previously (Giráldez et al., 2002; Wesch et al., 2012) using an

Table 1. Kinetic parameters of Kv7.2/3 currents

Expressed constructs	$V_{1/2}$ (mV)[a]	Slope (zF/RT)[a]	Activation constant (ms)[b]	Deactivation constant (ms)[c]
X. laevis oocytes				
Kv7.2/3	−31.6 ± 0.6 (n = 57)	8.8 ± 0.3 (n = 57)	102.8 ± 12.2 (n = 11)	55.3 ± 3.5 (n = 10)
Kv7.2/3 + SGK1.1	−31.1 ± 0.6 (n = 60)	9 ± 0.3 (n = 60)	140.4 ± 25.7 (n = 8)	42.6 ± 5.9 (n = 4)
HEK293				
Kv7.2/3	−21.27 ± 1.8 (n = 11)	13.8 ± 1.3 (n = 11)	80.4 ± 13.5 (n = 11)	43.3 ± 10.1 (n = 10)
Kv7.2/3 + SGK1.1	−19.43 ± 1.2 (n = 14)	14.98 ± 0.5 (n = 14)	72.3 ± 8.7 (n = 14)	49.2 ± 6.4 (n = 12)

[a]Half-maximal activation voltage calculated from Boltzmann equation fits to activation curves (Fig. 1*B*,*E*).

[b]Calculated from monoexponential fits to evoked currents at + 40 mV from −80 mV (oocytes) or −30 mV (HEK293).

[c]Calculated from monoexponential fits to evoked currents at −100 mV from holding potentials of + 50 mV (oocytes) or −30 mV (HEK293).

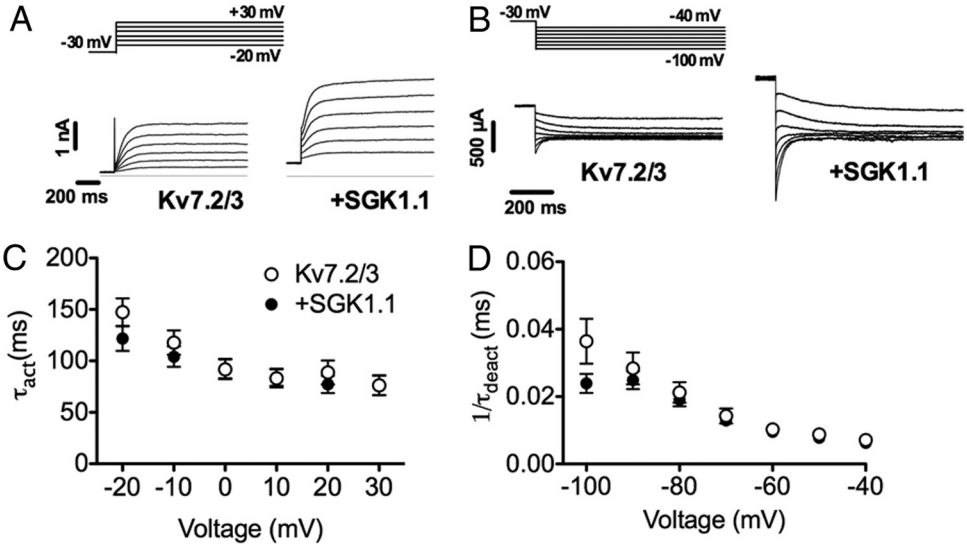

Figure 2. SGK1.1 does not modify the activation and deactivation kinetics of Kv7.2/3 channels. ***A***, Representative Kv7.2/3 current activation phase of Kv7.2/3 currents with or without SGK1.1 coexpression in HEK293 cells after depolarizing voltage steps ranging from −20 to +30 mV from a holding potential of −30 mV (inset). ***B***, Activation rate constant (τ_{act}) values obtained from monoexponential fits of current activation phase shown in ***A*** for the different voltages. Data points and error bars represent average ± SEM ($n \geq 11$). ***C***, Representative currents showing Kv7.2/3 deactivation phase after applying different hyperpolarizing pulses to voltages ranging from −40 to −100 mV from a holding of −30 mV (inset). ***D***, Deactivation rate time constant (τ_{deact}) of Kv7.2/3 currents with or without SGK1.1, obtained by monoexponential fitting of evoked current deactivation phase ($n \geq 10$).

Axopatch 700A patch-clamp amplifier (Molecular Devices). Patch pipettes with tip resistances of 3.5–5 MΩ were pulled from Kimax disposable micropipettes (Kimble Glass). The standard extra cellular saline contained the following (in mM): 137 NaCl, 4 KCl, 1.8 $CaCl_2$, 1 $MgCl_2$, 10 glucose, and 10 HEPES, pH 7.4 with NaOH. The internal pipette solution contained the following (in mM): 65 KCl, 30 K_2SO_4, 10 NaCl, 1 $MgCl_2$, 50 sucrose, and 10 HEPES, pH 7.4 with KOH. The tip of the pipette was initially filled with nystatin-free solution, and the remainder of the pipette was backfilled with the same solution containing 250 μg/ml nystatin (Sigma), added from a stock of 50 mg/ml nystatin freshly dissolved in DMSO. All nystatin-containing solutions were sonicated just before use. The course of perforation was followed by monitoring the progress of capacitive transients under voltage-clamp mode, setting the pipette voltage at a value of −70 mV. Access resistance, as estimated from the capacitive compensation circuitry on the amplifier, reached 10–30 MΩ within 5–20 min after the seal was made. Current density was calculated by dividing the current value at 50 mV by the cell membrane capacitance. Activation voltage-dependence curves and rates were obtained by depolarizing the cell from a holding potential of −30 mV to various pulses ranging from −120 to +80 mV for 1 s and measuring tail currents at a −30 mV pulse of 1 s. Deactivation was studied by applying hyperpolarizing pulses (ranging from −40 to −100 mV) from a holding potential of −30 mV.

Perforated-patch whole-cell recording of SCG neurons. SCG neurons were continuously perfused (~10 ml/min) at room temperature onto the plate of an inverted microscope. Pipettes of 2–4 MΩ containing freshly prepared 75 μg/ml amphotericin-B were used to perform perforated voltage- and current-clamp (*Iclamp-fast* simulating bridge mode) experiments (Magistretti et al., 1998) using an Axopatch 200B amplifier (Molecular Devices). Series resistances (≤20 MΩ) and junction potentials (≤5 mV) were not corrected (Rae et al., 1991; Neher, 1992). Voltage-clamp signals were sampled at 2 kHz and filtered at 0.5 kHz, whereas current-clamp experiments were sampled at 10 kHz and filtered at 5 kHz. The standard pipette solution contained the following (in mM): 90 K-acetate, 20 KCl, 3 $MgCl_2$, 1 $CaCl_2$, 3 EGTA, and 40 HEPES, adding ~20 NaOH to a pH of 7.2. Standard bath solution contained the following (in mM): 140 NaCl, 3 KCl, 1 $MgCl_2$, 2 $CaCl_2$, 10 D-glucose, and 10 HEPES, adjusted to pH 7.2 with Tris. Solutions were adjusted to 290–300 mOsm. The muscarinic agonist Oxo-M was applied to the perfusion system for 3 min. M-current inhibition was calculated by comparing the initial current ($t = 0$) to the maximal inhibition level, which was achieved in ~2 min. When recording A (I_A) and delayed rectifier ($I_{K(V)}$) currents the bath solution was complemented with TTX (0.5 μM), $CdCl_2$ (100 μM), and $CsCl_2$ (1 mM) to avoid contamination with sodium, calcium, and hyperpolarization-activated currents.

Data acquisition and analyses. Stimulation and data acquisition were controlled through a Digidata 1440A using pClamp 10.0 software (Molecular Devices). Data were plotted and analyzed using Clampfit (Molecular Devices), Igor Pro (Wavemetrics), and Prism (GraphPad Software). Activation curves were fitted to Boltzmann equations:

$$I = \frac{I_{max}}{1 + e^{\frac{(V - V_{1/2})}{k}}}$$

Activation and deactivation rates were measures by fitting a monoexponential curve to the evoked currents at indicated voltages.

Flow cytometry analyses

Flow cytometry was performed as described previously (Barroso-González et al., 2009; Gómez-Posada et al., 2011). Briefly, HEK293 cells transfected with the indicated DNA combinations were incubated with monoclonal antibody HA.11 (1:25 dilution; Covance) for 1 h at 4°C to avoid channel internalization. Then, cells were washed with ice-cold PBS and incubated with Alexa Fluor 488-conjugated anti-mouse IgG secondary antibody (Invitrogen) for 1 h at 4°C. After several washes in ice-cold PBS, cells were immediately analyzed by flow cytometry (XL-MCL system; Beckman Coulter). At least 3×10^4 cells from each sample were analyzed. Mean fluorescence intensity in linear scale was obtained adjusting the fluorescence gain so that <5% of the cells of the control sample were positive in the fluorescence channel. Negative controls consisted on nontransfected cells, nontransfected cells incubated with anti-HA.11, and cells transfected with Kv7.2/3–HA and incubated with an irrelevant antibody of the same isotype as HA.11 (anti-FLAG M2 IgG; Sigma).

KA-induced seizures

KA (Sigma) was dissolved in isotonic saline, pH 7.4, and administered intraperitoneally to adult age- and weight-matched C57BL/6 and Tg.SGK1 mice. After KA injections, mice were placed in clear plastic cages and monitored every 5 min for 2 h for motor activity and manifestations of limbic seizures (McCord et al., 2008). Mice were scored for seizure activity using a previously described scale (Racine, 1972). Racine stages were defined as follows: 1, immobility; 2, forelimb and/or tail extension, rigid posture; 3, repetitive movements, head bobbing; 4, rearing and falling; 5, continuous rearing and falling; 6, severe tonic–clonic seizures. In addition, latency of convulsions, duration of seizure activity and mortality were monitored.

Statistical analyses

Statistical analysis was performed using Prism software (GraphPad Software). Averages represent mean ± SEM, and the statistical significance was assessed with two-sample Student's *t* tests or one-way ANOVA, followed by Bonferroni's multiple-comparison test, for comparison of three or more groups.

Results

SGK1.1 increases Kv7.2/3 channel currents without affecting kinetic properties

Expression of Kv7.2 and Kv7.3 mRNA (Kv7.2/3) in *Xenopus* oocytes elicited non-inactivating voltage-dependent K^+ currents (Fig. 1*A*) as reported previously (Wang et al., 1998; Schwake et al., 2000). Coinjection of oocytes with Kv7.2/3 and equivalent quantities of SGK1.1 mRNA increased 2.6 times the Kv7.2/3 current measured at −20 mV after +30 mV step pulses (Fig. 1*C*). Half-maximal activation voltage ($V_{½}$), calculated after fitting voltage activation curves to Boltzmann equations (Fig. 1*B*, Table 1), remained unaffected by the kinase (Kv7.2/3, −31.6 ± 0.6 mV; Kv7.2/3 plus SGK1.1, −31.1 ± 0.6 mV). Likewise, SGK1.1 did not change the slope of the activation curves (Table 1). Therefore, the SGK1.1-mediated increase in current (Fig. 1*C*) could not be explained by a shift of the Kv7.2/3 voltage dependence of activation. We next tested whether the effect of the SGK1.1 on Kv7.2/3 currents depended on its phosphorylating activity by using an inactive mutant of SGK1.1 that substitutes a lysine residue (K220) in the ATP-binding cassette of the protein (Wesch et al., 2010). Coinjection of SGK1.1–K220A did not produce significant changes in current levels or activation curves (Fig. 1*A*, third panel, *B*,*C*), indicating that kinase activity of SGK1.1 is required for the increase in Kv2/3 current. A distinct char-

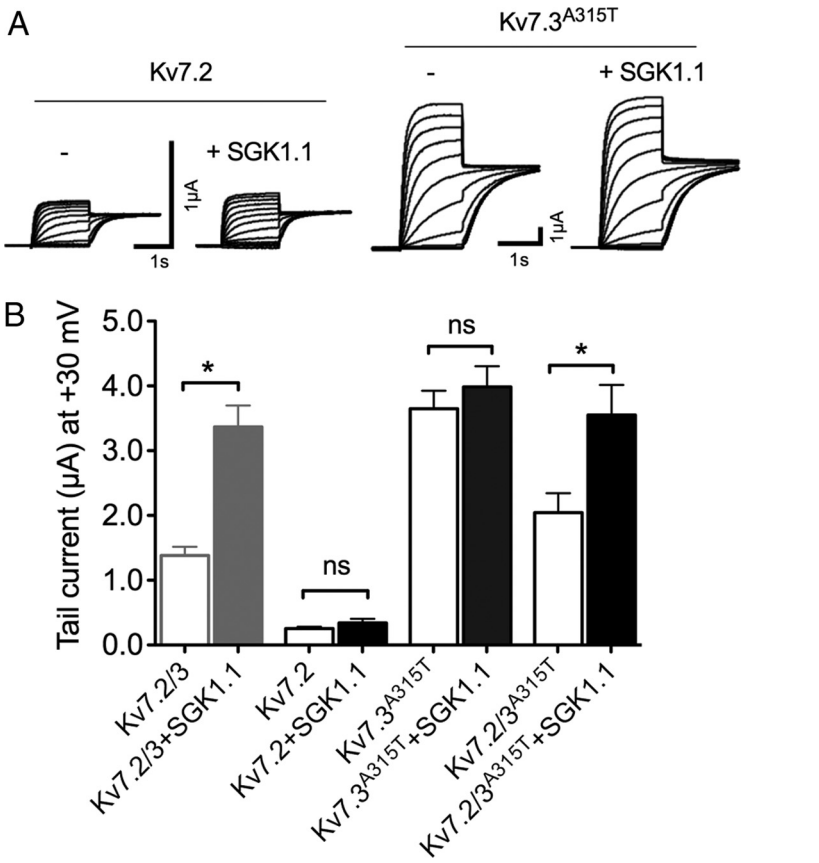

Figure 3. SGK1.1 requires the heteromers Kv7.2/3 to produce the increase in current. ***A***, Representative currents from *Xenopus* oocytes injected with Kv7.2 or Kv7.3–A315T (Kv7.3^{A315T}) mutants, obtained by sequential 10 mV step depolarizations ranging from −120 to +30 mV from a −80 mV holding potential. For clarity, only currents corresponding to −70 to +30 mV depolarizing pulses are shown. ***B***, Tail currents at +30 mV for indicated subunit combinations with and without SGK1.1 ($n \geq 20$, $n = 5$ batches). Values for Kv7.2/3 with or without the kinase from Figure 1 are shown in gray for reference. Data values were normalized to Kv7.2/3 current. *$p < 0.05$; ns, not significant.

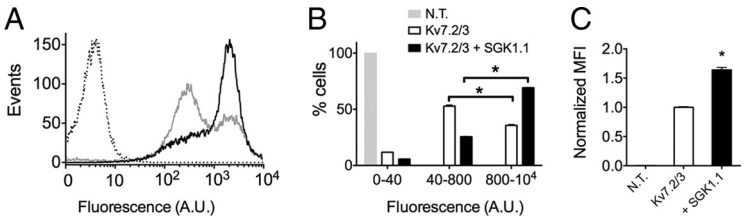

Figure 4. SGK1.1 increases Kv7.2/3 abundance in the cell surface. ***A***, Representative flow cytometry analysis showing cell-surface expression levels of Kv7.2–HA/Kv7.3–HA in HEK293 cells, without (gray histogram) or with (black histogram) SGK1.1. Punctuated-line histogram corresponds to nontransfected HEK293 cells (negative control). ***B***, Analysis graph representing percentage of cells showing fluorescence in the indicated intensity ranges. ***C***, Normalized mean fluorescence intensity (MFI) obtained in the 800 to 10^4 AU fluorescence region for nontransfected cells (N.T.) and cells transfected with Kv7.2/3 without (Kv7.2/3) or with (+SGK1.1) SGK1.1. Data correspond to two independent experiments performed in triplicate for Kv7.2/3 cotransfected cells with or without SGK1.1. *$p < 0.05$.

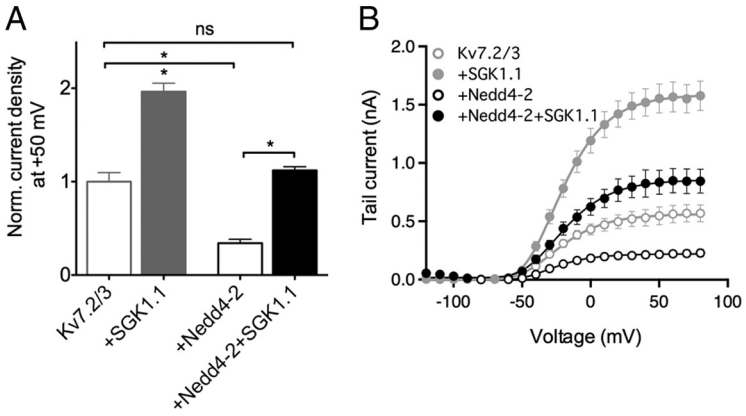

Figure 5. SGK1.1 regulation of Kv7.2/3 in HEK293 cells involves the Nedd4-2 signaling pathway. ***A***, Normalized tail currents at +50 mV for Kv7.2/3 with and without Nedd4-2 and/or SGK1.1 ($n \geq 6$) obtained in transfected HEK293 cells. Values for Kv7.2/3 with or without the kinase from Figure 1 are shown for reference (gray). Data values were normalized to Kv7.2/3 current magnitude. ***B***, Average activation curves and corresponding fits to Boltzmann equations (solid lines) for the construct combinations indicated in the graph legend ($n \geq 6$). Values corresponding to Kv7.2/3 with or without SGK1.1 from Figure 1 are shown for reference (gray). $^*p < 0.05$.

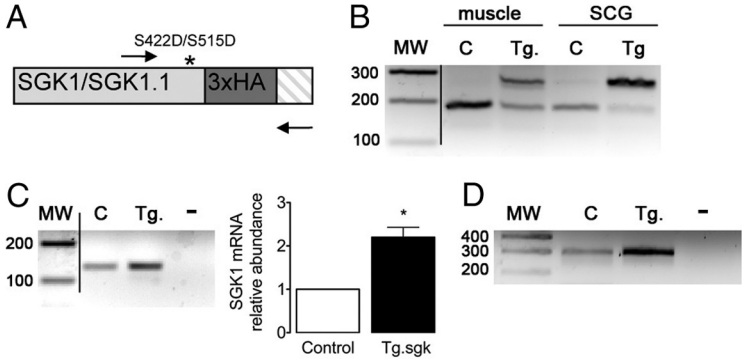

Figure 6. Expression of a constitutively active mutant of SGK1 in Tg mice SCGs. ***A***, Schematic representation of the 3′ end of Tg SGK1 isoforms mRNA, which includes a triple HA tag (dark gray box) and point mutation S422D (S515D in SGK1.1) that renders the kinase constitutively active (asterisk). Arrows indicate oligonucleotides used to simultaneously study the expression of endogenous and Tg SGK1. Crosshatched box indicates the 3′ untranslated region of the transcripts. ***B***, Agarose gel analysis of RT-PCR products obtained from skeletal muscle (tibialis anterior) or SCG from control (C) or Tg SGK1 mice using oligonucleotides flanking the 3′ end of SGK1 coding sequence, depicted in ***A***. MW, Molecular mass markers (values in base pairs). ***C***, Agarose gel analysis of RT-PCR products and qPCR analysis of total SGK1 transcript expression in control (C) or Tg SGK1 SCG. −, No template. Bars represent average ± SD abundance of SGK1 assessed by qPCR. $^*p < 0.05$. ***D***, RT-PCR products showing the expression of SGK1.1 isoform in control (C) and Tg SCG. −, No template.

acteristic of SGK1.1 is its localization at the plasma membrane because of a specific NH_2-terminal polybasic motif including residues K21, K22, and R23, which bind the kinase to PIP_2. Neutralization of these residues (with the substitutions K21N, K22N, and R23G; SGK1.1–KKR mutant) disrupts the membrane tethering of the kinase, leading to its retention in the cytoplasm (Arteaga et al., 2008; Wesch et al., 2010). We confirmed that membrane localization is necessary for SGK1.1-mediated modulation of Kv7.2/3 channel function, because coexpression of the channels with the SGK1.1–KKR mutant did not produce significant changes on Kv7.2/3 current levels or voltage dependence of activation (Fig. 1*A*, first panel, *B*, *C*).

To ensure that the effect of SGK1.1 on Kv7.2/3 channel function is a general regulatory mechanism not restricted to the *Xenopus* heterologous expression system, we also examined Kv7.2/3 currents in mammalian HEK293 cells. Currents elicited from HEK293 cells transfected with Kv7.2 and Kv7.3 DNA were similar to those reported in the literature (Nakajo and Kubo, 2005). As described previously for tsA201 cells (a variant of HEK293), we observed a shift of the voltage dependence of aperture in the rightward direction ($V_{½} = -21.27 \pm 1.8$ mV; Table 1) when compared with *Xenopus* oocytes (Shapiro et al., 2000). Coexpression of SGK1.1 with Kv7.2/3 channels in HEK293 cells produced a twofold increase in current magnitude (Fig. 1*D–F*), consistent with the effect observed in *Xenopus* oocytes. Similarly, the voltage dependence of activation was unchanged in cells coexpressing Kv7.2/3 channels and the kinase ($V_{½} = -19.43 \pm 1.2$; Fig. 1*E*, Table 1). Finally, we measured the effect of SGK1.1 on Kv7.2/3 activation and deactivation rate constants. As shown in Figure 2, rates were not modified by coexpression of SGK1.1 at any voltage tested in HEK293 cells (Fig. 2, Table 1). Analogous results were observed in *Xenopus* oocytes (Table 1).

Together, our results show that the increase in Kv7.2/3 current induced by SGK1.1 is not attributable to changes in the kinetic properties of Kv7.2/3 channels, suggesting that it could be attributable to enhanced plasma membrane abundance.

SGK1.1 effect requires the heteromultimeric assembly of Kv7.2/3 channels

Although the M-current is predominantly mediated by coassembly of Kv7.2 and Kv7.3 isoforms, it has also been suggested that Kv7.2 homomultimers could underlie M-current in certain regions of the CNS (Schwarz et al., 2006). Thus, we explored the subunit specificity of the SGK1.1 effect. As described previously (Wang et al., 1998), we obtained current amplitudes for homomeric Kv7.2 channels that were ~10-fold smaller than those of Kv7.2/3. In this case, coexpression with SGK1.1 did not cause any change in current amplitude (Fig. 3*A*, left two panels, *B*) or other kinetic parameters (data not shown). As reported previously (Wang et al., 1998), we observed no detectable currents from Kv7.3 homomers expressed in oocytes. Coexpression of SGK1.1 with Kv7.3 did not induce detectable currents (data now shown). Thus, we used a previously described mutation (A315T) in the pore of Kv7.3 that greatly increases membrane expression and current amplitude by altering the pore structure (Etxeberria et al., 2004; Zaika et al., 2008; Gómez-Posada et al., 2010). As seen in Figure 3, Kv7.3–A315T produced much larger currents than Kv7.2, Kv7.3, or Kv7.2/3 multimers. Nevertheless, SGK1.1 did not affect Kv7.3–A315T current levels significantly (Fig. 3*B*). To address the hypothesis that the A315T mutation could be masking the effect of SGK1.1, we coexpressed Kv7.2 with Kv7.3–A315T and tested whether SGK1.1 was able to increase current levels. The results demonstrate that heteromers formed by Kv7.2/Kv7.3–A315T respond normally to SGK1.1 stimulation (Fig. 3*B*). Overall, these results indicate that SGK1.1 is only effective when

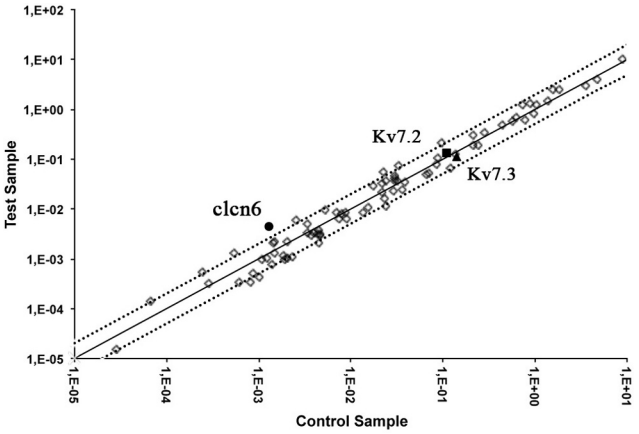

Figure 7. Analysis of relative mRNA expression changes of relevant neuronal ion channels and transporters between wild-type and Tg.SGK1 animals in SCGs. Scatter plot values are expressed as $2^{-\Delta Ct}$. Dotted lines indicate an arbitrary twofold change in gene expression threshold. Filled circles, clcn6; filled squares, Kv7.2; filled triangles, Kv7.3. Genes analyzed and found to have fold changes in expression ≤2: Accn1, Accn2, Accn3, Atp1a1, Atp1b1, Atp1b2, Atp4a, Atp5b, Atp6ap1, Atp6v0b, Cacna1a, Cacna1b, Cacna1c, Cacna1 g, Cacna1h, Cacnb1, Cacnb2, Cacnb3, Cacnb4, Cacng2, Clca1, Clcn1, Clcn2, Clcn3, Clcn4–2, Clcn5, Clcn7, Clic1, Kcna1, Kcna2, Kcna3, Kcna6, Kcnb1, Kcnc1, Kcnc3, Kcnc4, Kcnd1, Kcnd2, Kcnd3, Kcne1, Kcnh1, Kcnh2, Kcnj15, Kcnj3, Kcnj8, Kcnmb1, Kcnn1, Kcnn2, Kcnn3, Kcnn4, Kcnq1, Kcnq2, Kcnq3, Kcnq4, Kcns1, Kcns2, Kcns3, Scn1a, Scn1b, Scn3a, Scn4a, Scn5a, Scn7a, Scn8a, Scn9a, Slc1a1, Slc6a12, Slc6a3, Slc6a9, and Vdac1. Genes analyzed but found to be not expressed in the samples: Cacna1s, kcna5, kcnj4, and Slc18a3. Genes analyzed but resulting in unreliable results (>1 peak in melting temperature analysis): Atp2a1, Cftr, Kcna4, Kcnf1, Kcnh3, Kcnj1, Kcnj4, Kcnj5, Kcnj6, and Kcnj11.

Kv7.2 and Kv7.3 channels are forming heteromultimers at the plasma membrane.

SGK1.1 increases Kv7.2/3 surface expression

It has been reported that SGK1.1 increases the activity of some ion channel types by augmenting membrane abundance through changes in channel trafficking (Arteaga et al., 2008; Wesch et al., 2010). We tested whether this was the case for Kv7.2/3 by using flow cytometry to quantify membrane surface expression of Kv7.2/3 channels labeled with an HA extracellular epitope (Gómez-Posada et al., 2011). Coexpression of SGK1.1 with Kv7.2/3 channels in HEK293 cells lead to a significant increase in cell-surface expression of the channel (Fig. 4). Controls using HA antibody in nontransfected cells or an irrelevant antibody of the same isotype (anti-FLAG IgG1 antibody) in cells transfected with Kv7.2/3–HA did not result in fluorescent signals above background (data not shown). Cells transfected with Kv7.2/3–HA showed a biphasic distribution of cell-surface fluorescence intensity, with ~60% of the cells in the population with lower channel plasma membrane abundance (Fig. 4*A*, gray trace, *B*, *C*, white bars). Expression of SGK1.1 produced a more homogenous cell population (~75% in the higher plasma membrane abundance; Fig. 4*A*, black trace, *B*, *C*, black bars). This increase in cell membrane abundance is consistent with the higher current levels produced by SGK1.1, indicating that the increased surface expression of the channel accounts for the augmented current.

SGK1.1 regulation involves the Nedd4-2 pathway

Schuetz et al. (2008) proposed that the ubiquitous SGK1 regulates surface levels of Kv7.2/3 channels by phosphorylation and consequent inactivation of the ubiquitin-ligase Nedd4-2, which otherwise would lead to channel internalization. This mechanism has been also proposed for SGK1 regulation of other ion channels (Debonneville et al., 2001; Snyder et al., 2002). To test whether the neuronal isoform SGK1.1, with distinctive properties and membrane-specific subcellular localization, also involves the Nedd4-2 pathway in mammalian cells, we coexpressed Kv7.2/3 in HEK293 cells with combinations of Nedd4-2 with or without SGK1.1. As observed previously in *Xenopus* oocytes (Ekberg et al., 2007), Nedd4-2 significantly decreased Kv7.2/3 current levels to 34 ± 4% of control levels (Fig. 5*A*,*B*). Similarly to previous findings (Ekberg et al., 2007), we did not observe Nedd4-2-induced decrease in current when the Kv7.2 or Kv7.3 subunits were expressed alone in HEK293 cells (data not shown). When SGK1.1 and Nedd4-2 were coexpressed with Kv7.2/3 channels, there was no significant change on current levels (Fig. 5*A*). Nedd4-2 alone or coexpressed with SGK1.1 had no effect on Kv7.2/3 voltage dependence of activation (Fig. 5*B*), nor in deactivation or activation rates (data not shown). These findings are consistent with SGK1.1 phosphorylating and inactivating the overexpressed Nedd4-2, resulting in no change on Kv7.2/3 channels surface expression.

Constitutively active SGK1.1 induces an increase in M-current levels and diminished electrical excitability of sympathetic neurons

To study whether the regulatory effect of SGK1.1 is conserved in the physiological context of a neuron, we measured M-current amplitude in SCG cells isolated from a Tg mouse model (Tg.sgk) expressing near-physiological levels of a constitutively active mutant of all SGK1 splicing variants (S422D in SGK1, S515D in SGK1.1).

We confirmed the expression of the transgene in SCG by RT-PCR using a set of primers flanking the triple HA tag inserted in the COOH terminus of Tg SGK1 (Fig. 6*A*). The results showed the expected pattern of two bands corresponding to the endogenous and the Tg expression of HA-labeled SGK1 (Fig. 6*B*). Samples from control animals only displayed the lower band corresponding to the endogenous gene. Other tissues, such as skeletal muscle, also showed expression of the transgene, as expected from the known ubiquitous expression of SGK1 (Fig. 6*B*). The amount of SGK1 transcript expressed in SCG of control and Tg animals was studied by RT-PCR and qPCR (Fig. 6*C*). The results showed a twofold increased expression of SGK1 in Tg mice, consistent with the use of a BAC containing the physiological SGK1 promoter instead of a construct overexpressing the cDNA. Using SGK1.1 isoform-specific primers, we confirmed the expression of this isoform in SCG and the increased amount present in Tg mice (Fig. 6*D*). Given that SGK1.1 protein stability is one order of magnitude higher than that of SGK1 (Arteaga et al., 2008; Raikwar et al., 2008), SGK1.1 is the predominant isoform expressed in neurons (Arteaga et al., 2008).

Some SGK1 isoforms have been shown previously to phosphorylate and control the activity of members of the FoxO family of transcription factors (Brunet et al., 2001) (Arteaga et al., 2007). To examine the effect of constitutive expression of the Tg SGK1.1–S515D in the expression of ion channels involved in the regulation of membrane potential and excitability, we used a commercial PCR array to analyze 75 different neuronal ion channels and transporters (for a complete list of analyzed genes, see legend for Fig. 7). Comparison of gene expression levels between control and Tg.sgk SCGs revealed that most genes varied by a factor of ≤2 (Fig. 7). Kv7.2 and Kv7.3 variation between control and Tg animals was <20%. Only one mRNA, coding for the neuronal lysosomal chloride transport protein CLCN-6, for which no significant role in neuronal function has been reported (Poët et al., 2006), showed 3.4-fold higher expression in Tg.sgk

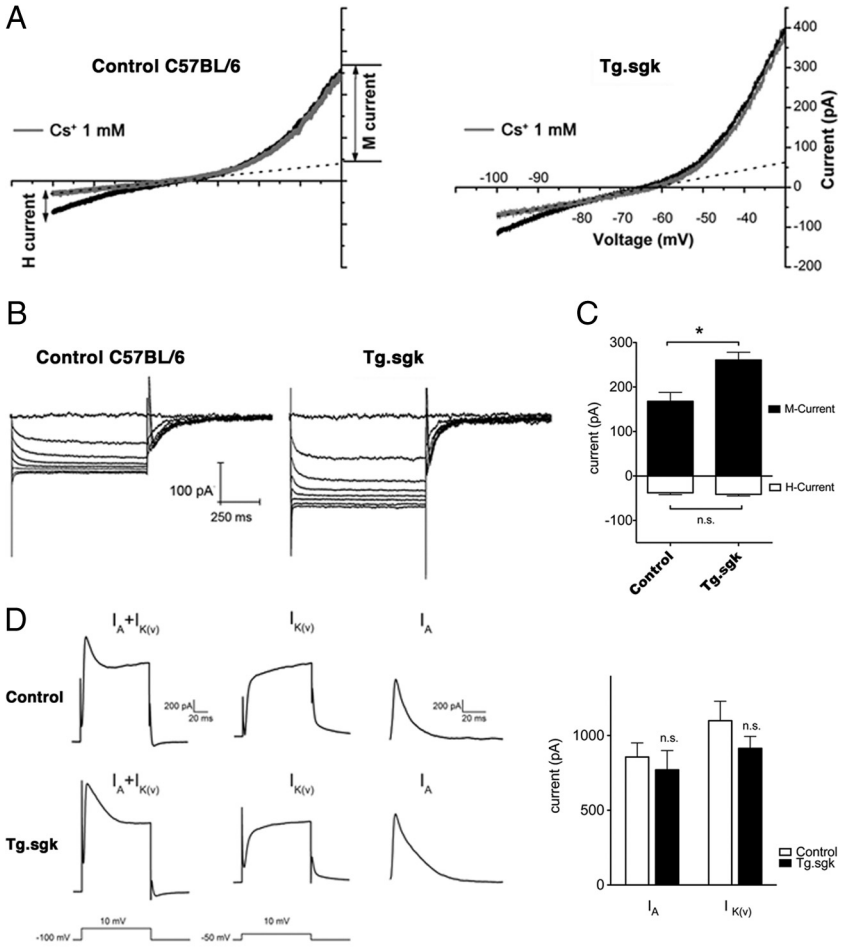

Figure 8. SCG neurons isolated from Tg.sgk mice show a significant increase in M-current. ***A***, Representative voltage-ramp current responses elicited from SCG neurons isolated from control C57BL/6 mice (left) and Tg.sgk mice (right) before (black line) and after (gray line) adding 1 mM Cs. M-current amplitude at −30 mV was measured by subtracting the leak from the total current. The amplitude of the leak current was determined from extrapolated current–voltage curves (dotted line). ***B***, M-currents in response to 2 s voltage steps (−30 to −100 mV in 10 mV increments) in control mice neurons (left) and in Tg.sgk neurons (right). ***C***, Average M-current (positive, black bars) and H-current (negative, white bars) in neurons isolated from control mice ($n = 17$) and from Tg mice ($n = 21$). Error bars represent the SEM. *$p < 0.05$; ns, not significant. ***D***, Left, Representative current traces elicited from control (top) and Tg.sgk (bottom) SCG neurons in response to the voltage pulses indicated below the traces. Right, Average I_A and $I_{K(V)}$ current values corresponding to SCG neurons isolated from control (white bars) and Tg.sgk (black bars) mice.

ganglia versus control animals (Fig. 7). Together, the results suggest that long-term SGK1.1 hyperactivity does not induce significant changes in mRNA expression of ion channels involved in neuronal excitability.

The amplitude of the M-current at −30 mV was measured in cultured SCG neurons isolated from transgenic Tg.sgk mice and compared with that obtained in control animals with the same genetic background (C57BL/6). Voltage ramps to −100 mV from a holding potential of −30 mV (10 mV/s) were repetitively applied to follow M-current evolution (Fig. 8*A*). We applied Cs^+ (1 mM) to both subtract the leak current from the ramps and also measure H-current as the Cs^+-sensitive current (Lamas, 1998; Lamas et al., 2002; Romero et al., 2004). SCG neurons from Tg.sgk mice showed ~1.6-fold larger M-currents than control mice (Tg.sgk, 260.7 ± 17.4 pA; C57BL/6, 167.8 ± 20.1 pA; Fig. 8*C*). This increase in current magnitude occurred without apparent variations in other properties of the M-current (Fig. 8*B*). H-current levels were measured at negative voltages (−100 mV) by subtracting currents before and after 1 mM Cs^+ addition (Lamas et al., 2002) and were not affected by the activity of the kinase (C56BL/6 mice, −40.2 ± 3.9 pA; Tg.sgk mice, −37.8 ± 4.0 pA; Fig. 8*C*). Because other voltage-dependent potassium currents have been shown to be modulated by SGK1 (Henke et al., 2004), we decided to measure the outward A and delayed rectifier currents in control and Tg SCG neurons (Fig. 8*D*). To isolate the A-current, neurons were depolarized to 10 mV first from a holding potential of −100 mV and then from a holding of −50 mV. The first protocol activates both currents, the second one activates only the delayed rectifier, and the A-current was obtained by digitally subtracting these two responses as described in Figure 8*D*. Neither A (control, 856.7 ± 94.5 pA; Tg.sgk, 769.9 ± 129.5 pA) nor delayed rectifier (control, 1099.8 ± 129.7 pA; Tg.sgk, 914.8 ± 79.6 pA) current amplitudes were significantly affected in Tg mice ($n = 9$, controls; $n = 11$, Tg.sgk). These results strongly suggest that the actions of SGK1.1 are specific to the M-current.

Enhanced M-currents lead to decreased cellular excitability (Brown and Adams, 1980; Marrion, 1997; Romero et al., 2004). Thus, we speculated that the higher M-current levels observed in Tg.sgk mice should translate into reduced SCG neurons excitability. We assessed the effect of enhanced SGK1.1 activity on the spike frequency adaptation, typical of SCG neurons (Fig. 9*A*), by measuring the number of action potentials in response to 1 s depolarizing current injections of increasing amplitude (Fig. 9*B*). Consistent with the observed increase in M-current amplitude, Tg.sgk–SCG neurons fired a significantly lower number of action potentials after injecting depolarizing steps below 250 pA (Fig. 9*A*,*B*). Moreover, SCG cells from Tg.sgk mice showed a shift toward more negative resting potentials (Tg.sgk, −62.5 ± 1.8 mV; C57BL/6, −58.9 ± 1.6 mV), supporting the idea that the higher SGK1.1 activity in the Tg mice SCG leads to decreased neuronal excitability by an increase in the resting potassium conductance.

Individual action potential characteristics, such as amplitude and duration, were analyzed and found to be indistinguishable between Tg.sgk and wild-type cells (Table 2). This suggests that ion channels participating in the generation of action potentials are not affected in Tg neurons, reinforcing the idea that, at least in these cells, the action of SGK1.1 is specific to the M-current. Also, the latency to the first action potential remained unchanged (Table 2), which is compatible with the slow activation of M-currents (Cadaveira-Mosquera et al., 2011).

Muscarinic receptor activation counteracts SGK1.1 effect on M-currents

M-current is strongly inhibited in sympathetic ganglia by muscarinic agonists that, after binding to M_1 receptors at the membrane

(Marrion et al., 1989), activate cytoplasmic phospholipase C (PLC) and PIP_2 hydrolysis. It has been proposed that any receptor or pathway that couples to this cascade will control the M-current (Marrion, 1997) ultimately by PIP_2 depletion (Kosenko et al., 2012). SGK1.1 has been implicated recently in PLC-mediated signaling through activation of G-protein-coupled receptors (GPCRs; Wesch et al., 2010). Thus, we evaluated the role of SGK1.1 in M-current muscarinic inhibition. We tested the effect of increased SGK1.1 activity on M-current muscarinic inhibition in SCG neurons from Tg.sgk mice. As seen in Figure 10, *A* and *B*, M-current inhibition by Oxo-M was significantly higher in Tg.sgk–SCG neurons (C57BL/6 mice, 45.6 ± 3.8%; Tg.sgk mice, 66.5 ± 6%). Interestingly, both Tg.sgk and control SCG neurons reached similar current levels after treatment with the muscarinic agonist (control, 77.6 ± 10.1 pA; Tg.sgk, 75.8 ± 19.9 pA). Because SGK1.1 is bound to PIP_2, M-current reduction by Oxo-M in Tg.sgk neurons may be attributable to the synergistic disappearance of the kinase from the membrane and loss of channel function after PIP_2 depletion. The putative contribution of SGK1.1 translocation from the membrane to the M-current reduction might be suggested by comparing the time course of the muscarinic response between control and Tg.sgk neurons. We observed no significant difference in the time needed to reach maximal inhibition current levels after Oxo-M addition (control, 137.2 ± 15.2 s, $n = 11$; Tg.sgk, 105 ± 8.7 s, $n = 10$). This result suggests that loss of channel function by PIP_2 depletion as the main mechanism underlying M-current reduction in both cases.

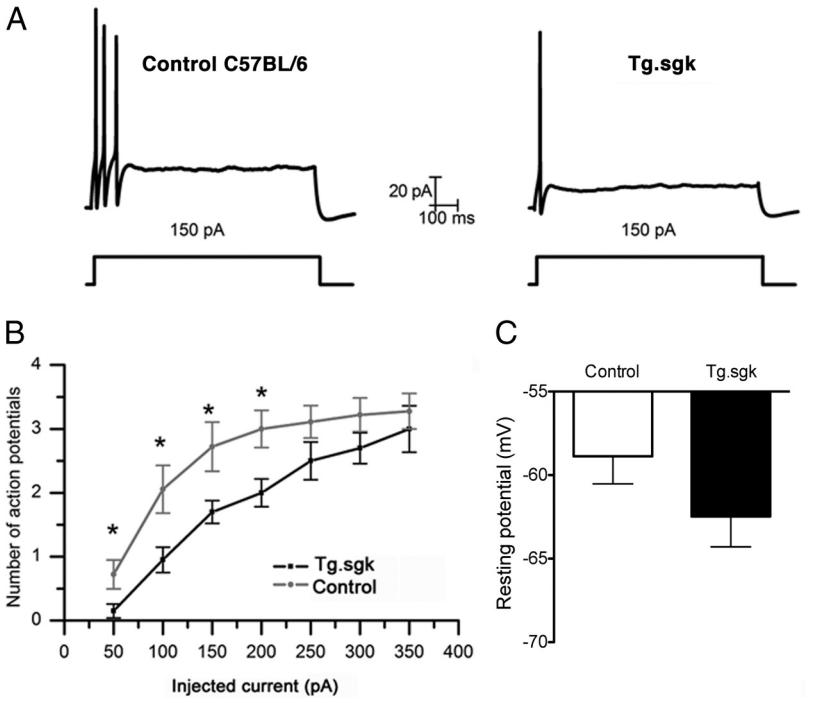

Figure 9. SCG neurons from Tg.sgk mice show more negative resting potentials and less excitability. ***A***, Representative action potential recordings in response to a 150 pA pulse in SCG neurons isolated from control mice C57BL/6 (left) and Tg.sgk transgenic mice (right). ***B***, Representation of the average number of action potentials generated in response to stimulus of different amplitude (picoamperes) for control mice (gray line) or Tg.sgk–SCG neurons (black line). ***C***, Average resting membrane potential measured in SCG neurons isolated from control mice (white bar, $n = 20$) and Tg mice (black bar, $n = 18$). $^*p < 0.05$.

Altogether, our results indicate that, in SCG neurons, SGK1.1 can modulate the M-current, thus regulating the resting membrane potential and neuronal firing properties. Moreover, the effect of SGK1.1 on M-current is fully reversed by muscarinic agonists and therefore provides a convergent pathway depending on PIP_2 levels for the regulation of electrical activity in neurons.

Tg SGK1 mice show diminished response to KA-induced seizures

In view of our results, it is tempting to hypothesize that decreased neuronal excitability attributable to enhanced SGK1.1 activity in the CNS should render Tg mice more resistant to chemically induced seizures. To test this idea, we used the KA-induced seizure model of generalized neuronal hyperexcitability. Systemic administration of KA produces a well-characterized pattern of seizure activity that is sustained for several hours. Two-month-old control (C57BL/6) and Tg.sgk mice were treated with three different doses of KA (15, 20, and 25 mg/kg). Preliminary experiments showed the absence of seizure activity with a 15 mg/kg treatment, consistent with previously published data for this mouse strain and age (McCord et al., 2008). Treatment with 20 or 25 mg/kg KA did not show any significant difference, and therefore the data from both treatments were pooled. In both genotypes, 90% of animals initially responded to KA intraperitoneal injection with immobility (Racine stage 1; Racine, 1972), with no difference in onset time between control and Tg.sgk. However, the number of animals that progressed from stage 1 through stage 6 was significantly different (Fig. 11). A total of 55% of controls reached Racine stage 6, and the treatment was lethal for 44% of them. In contrast, only 9% of Tg animals displayed seizure activity (stage 6) after KA injection, and none died (Fig. 11). These results are consistent with a neuroprotective effect of reduced excitability of Tg.sgk mice attributable to increased SGK1.1 activity.

Table 2. Action potential parameters in SCG neurons

	AP amplitude (mV)	AP duration (ms)	AP latency (ms)
Control	80.7 ± 2.7 ($n = 7$)	1.31 ± 0.06 ($n = 7$)	35.3 ± 6.3 ($n = 7$)
Tg.sgk	82.2 ± 3.2 ($n = 9$)	1.2 ± 0.1 ($n = 9$)	40.23 ± 12.02 ($n = 8$)

AP, Action potential.

Discussion

Our work shows that the neuronal SGK1.1, with distinct subcellular localization and properties, regulates M-current in heterologous expression systems and in SCG neurons, in which it modulates cell excitability. Moreover, Tg mice displaying enhanced SGK1.1 activity in the CNS are resistant to chemically induced seizures, arguing in favor of a role for SGK1.1 in the regulation of neuronal excitability.

SGK1.1 is a neuronal isoform that was initially detected in human and mouse brain (Arteaga et al., 2008; Raikwar et al., 2008). Although its transcript abundance is ~1/10 lower than SGK1 in neurons, SGK1.1 is the most prominent isoform in neurons at the protein level because of its enhanced stability (Arteaga et al., 2008). In addition, SGK1.1 shows a distinct subcellular localization that turns it into a potential physiological player in

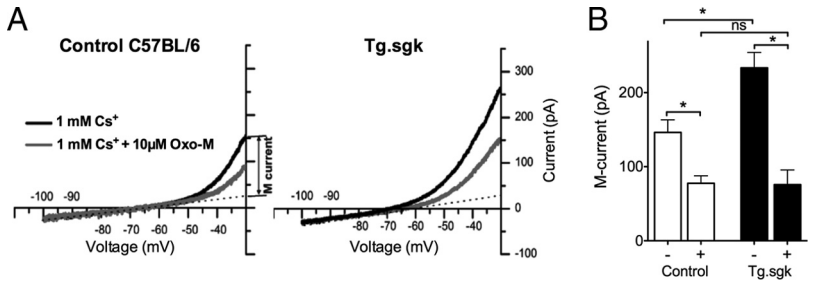

Figure 10. Muscarinic activation counteracts SGK1.1 effect on Kv7.2/3 currents. ***A***, Representative current responses to voltage ramps elicited in SCG neurons isolated from control C57BL/6 (left) and Tg.sgk (right) mice before (black line) and after (gray line) adding 10 μM Oxo-M. All recordings were done in 1 mM Cs^+. Dotted line represents the extrapolated current–voltage leak current used to calculate M-current values. ***B***, Average M-currents before (−) and after (+) Oxo-M addition from SCG neurons isolated from control C57BL/6 ($n = 10$) and from transgenic Tg.sgk mice ($n = 11$). *$p < 0.05$; ns, not significant.

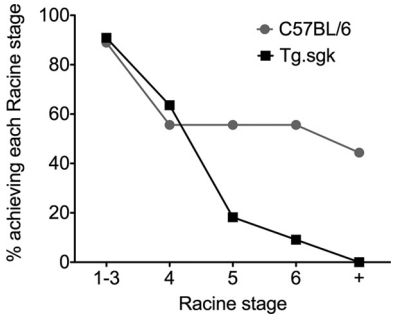

Figure 11. Tg sgk mice are resistant to KA-induced seizure activity. Plot represents percentage of control mice (C57BL/6; $n = 9$) or Tg.sgk mice ($n = 11$) that reached the indicated Racine stages (stage 6 defined as severe tonic–clonic seizures). + indicates death.

neuronal Kv7.2/3 channel regulation. It resides at the plasma membrane by binding to PIP_2 (Arteaga et al., 2008; Wesch et al., 2010), a phospholipid that constitutes the primary controller for M-channel activity (Delmas and Brown, 2005). Recently, it has been shown that the non-neuronal, ubiquitously expressed isoform SGK1 regulates Kv7.2/3 channels in *Xenopus* oocytes (Schuetz et al., 2008). Altogether, these precedents provided motivation for the present study, in which we have investigated the role of neuronal SGK1.1 in M-current modulation.

Our results demonstrate that Kv7.2/3 currents are increased by SGK1.1 by a regulatory mechanism that is not exclusive of *Xenopus* oocytes but it is also present in mammalian expression systems (HEK293). Furthermore, we observe equivalent effects on M-currents of SCG neurons from Tg mice expressing a constitutively active form of SGK1.1 (Arteaga et al., 2007). In all systems studied, SGK1.1 increases current levels to approximately twofold, without altering Kv7.2/3 voltage dependence of activation, the slope of the activation curve, or the channel activation or deactivation rates, suggesting that the mechanism underlying the current increase may be related to channel trafficking. Flow cytometry has been used previously to study Kv7.2/3 membrane abundance levels (Gómez-Posada et al., 2011). Using this technique, we show that the observed Kv7.2/3 current increase can be fully accounted for by an increment in the channel membrane levels. This is consistent with other regulatory roles of SGK1.1, such as modulation of plasma membrane abundance of ASIC1 and δ-ENaC channels (Arteaga et al., 2008; Wesch et al., 2010).

In other cell contexts, the related kinase SGK1 has been shown to increase protein membrane abundance by phosphorylating and inactivating the Nedd4-2 E3 protein ubiquitin ligase, thus reducing protein internalization through the ubiquitination pathway (Debonneville et al., 2001; Snyder et al., 2002). In *Xenopus* oocytes, it has been proposed that regulation of Kv7.2/3 by ubiquitously expressed SGK1 involves Nedd4-2 through a PY-independent pathway (Ekberg et al., 2007; Schuetz et al., 2008). Interestingly, neuronal SGK1.1 has been involved in regulation of ASIC and δ-ENaC channels that lack PY motifs, although participation of Nedd4-2 was not directly tested (Arteaga et al., 2008; Wesch et al., 2010). In this work, and for all systems studied to date, we observe a reduction in Kv7.2/3 current levels when Nedd4-2 is coexpressed, consistent with this ubiquitin ligase increasing the retrieval of channels from the membrane. This current reduction does not occur when Nedd4-2 is coexpressed with SGK1.1, and the most plausible explanation is that inactivation of overexpressed Nedd4-2 by SGK1.1 phosphorylation abrogates the effect of the ubiquitin ligase and results in current levels that are indistinguishable from cells expressing solely Kv7.2/3 channels. This effect strongly depends on the amount of Nedd4-2 plasmid transfected (data not shown), supporting the hypothesis that SGK1.1 and Nedd4-2 balance regulates Kv7 membrane abundance.

Our data also show that SGK1.1 functions exclusively on Kv7.2/3 heteromers, with no effect on Kv7.2 or Kv7.3 homomers. It is known that Kv7.2/3 heteromers are more efficiently trafficked to the membrane (Schroeder et al., 1998; Wang et al., 1998; Etxeberria et al., 2004). Proposed mechanisms underlying this regulation are the uncovering of otherwise hidden forward trafficking motifs or the concealing of functional endoplasmic reticulum retention signals (Schwake et al., 2003, 2006; Etxeberria et al., 2004). Other regulation mechanisms, such as the muscarinic pathway, have been reported to modulate Kv7.3 or Kv7.2 individually, albeit slightly less strongly than Kv7.2/3 heteromultimers (Shapiro et al., 2000). To overcome the fact that Kv7.3 homomers produced undetectable currents, we used the Kv7.3–A315T mutants, which produce significantly larger Kv7.3 currents. Our observation that SGK1.1 does not modify Kv7.3–A315T current levels but does increase Kv7.2/Kv7.3–A315T currents strongly suggests that there is no effect of the kinase on Kv7.3 homomers. These results are consistent with our finding in HEK293 cells that the Nedd4-2-mediated decrease in Kv7.2/3 currents only occurs when the heteromers are expressed and not with Kv7.2 or Kv7.3 homomers. This has been reported previously in *Xenopus* oocytes for the regulation of Kv7.2/3 and Kv7.3/5 heteromers by SGK1 (Ekberg et al., 2007). Our results argue in favor of the idea that, to be optimally internalized by Nedd4-2, the C-terminal regions of Kv7.2 and Kv7.3 must form a specific interaction, which could involve accessory proteins (Tinel et al., 2000; Gamper et al., 2005).

Our work shows an SGK1.1-driven increase of M-current in neurons isolated from mice SCG, in which such currents are produced by Kv7.2/3 heteromers (Hadley et al., 2003). In these neurons, Kv7 channels are responsible for resting potential maintenance and spike frequency adaptation (Romero et al., 2004). Although Tg.sgk mice express all SGK1 isoforms, the specific increase in neuronal M-currents is most likely attributable to SGK1.1 function, because this is the predominant, highly stable isoform in neurons (Arteaga et al., 2008; Raikwar et al., 2008).

Our results show that SGK1.1 acts specifically on M-currents, without altering H-current, A-current, or delayed rectifier K^+ channel current levels. In addition, the amplitude and duration of action potentials did not vary in Tg.sgk–SCG neurons when compared with wild-type cells, suggesting that voltage-dependent sodium and calcium channels are not strongly affected. Furthermore, mRNA expression of a variety of ion channels involved in neuronal excitability (see legend to Fig. 7) did not change between Tg.sgk and wild-type animals. Only a modest increase in CLCN-6 transcript abundance was observed. Genetic ablation of this lysosomal chloride transporter in mice produces no apparent phenotype or neuronal defects, and the physiological role of this transporter remains unclear (Poët et al., 2006). We cannot discard that other ion channels unrelated to neuronal excitability are altered at the mRNA or functional level. Our results in SCG neurons paralleled our findings in heterologous expression systems and are consistent with an increase of Kv7.2/3 membrane abundance levels rather than modification of M-current kinetic characteristics.

What is the physiological significance or SGK1.1 regulatory mechanism? The M-current is the basis of cellular excitability in many neuronal cell types because of its activation at resting potentials, thus contributing to the resting conductance and input cell resistance (Jentsch, 2000). In fact, merely a 25% decrease in M-current is enough to drive human neurons to epileptogenic levels causing neonatal epilepsy (Schroeder et al., 1998). Physiologically, M-current is regulated by mechanisms involving changes in PIP_2 levels, such as the GPCR regulatory pathways, because binding of this phospholipid activates the channel (Brown and Adams, 1980; Marrion, 1997; Shapiro et al., 2000; Delmas and Brown, 2005; Zaika et al., 2006; Hernandez et al., 2008). Replenishment of the phospholipid by activation of the 1-phosphatidylinositol 4-kinase (PI4K; Loew, 2007) must occur to recover current levels after muscarinic inhibition (Suh and Hille, 2002). Activation mechanisms for PI4K include PIP_2 depletion through phosphatidylinositol transfer protein activation (Gehrmann and Heilmeyer, 1998) and PKC activation through membrane depolarization (Chen et al., 2011). The latter has been shown to increase Kv7.2/3 currents in *Xenopus* oocytes (Zhang et al., 2010). We suggested recently that the neuronal, membrane-linked SGK1.1 constitutes a novel ion channel function regulator coupled to PLC and GPCR (Wesch et al., 2010). We now demonstrate that SGK1.1 upregulates M-current not only in heterologous systems but also in SCG neurons isolated from Tg mice, with a concomitant reduction in cell excitability. Interestingly, SGK1.1 transcription levels are increased after membrane depolarization (Arteaga et al., 2008), which has been also proposed to increase PIP_2 membrane levels (Chen et al., 2011). This would provide a mechanism for rapid recruitment of SGK1.1 to the membrane, in which it would upregulate M-current, contributing to recover baseline membrane potential. Moreover, SGK1.1-mediated activation of M-current is totally counteracted by muscarinic activation, a mechanism that would restore M-current levels. Therefore, PIP_2 levels, balanced by the action of depolarization, PLC-coupled receptors, and PI4K (Falkenburger et al., 2010b), provide a coincidence point for SGK1.1 localization and Kv7.2/3 regulation.

The SGK1.1-mediated enhancement of M-current in SCG neurons is paralleled by a significantly lower number of induced action potentials and a shift of the resting potential toward more negative values (farther from threshold), consistent with reduced neuronal excitability. Tg mice with enhanced SGK1.1 activity are resistant to the development of KA-induced seizures, which occur mainly in the temporal lobe (Lothman and Collins, 1981; Buckmaster, 2004). Altogether, our results provide evidence for SGK1.1 as a novel regulatory mechanism to counteract hyperexcitability in central neurons.

References

Alvarez de la Rosa D, Zhang P, Náray-Fejes-Tóth A, Fejes-Tóth G, Canessa CM (1999) The serum and glucocorticoid kinase sgk increases the abundance of epithelial sodium channels in the plasma membrane of *Xenopus* oocytes. J Biol Chem 274:37834–37839. CrossRef Medline

Arteaga MF, Alvarez de la Rosa D, Alvarez JA, Canessa CM (2007) Multiple translational isoforms give functional specificity to serum- and glucocorticoid-induced kinase 1. Mol Biol Cell 18:2072–2080. CrossRef Medline

Arteaga MF, Coric T, Straub C, Canessa CM (2008) A brain-specific SGK1 splice isoform regulates expression of ASIC1 in neurons. Proc Natl Acad Sci U S A 105:4459–4464. CrossRef Medline

Barros F, Gomez-Varela D, Viloria CG, Palomero T, Giráldez T, de la Peña P (1998) Modulation of human erg K^+ channel gating by activation of a G protein-coupled receptor and protein kinase C. J Physiol 511:333–346. CrossRef Medline

Barroso-González J, El Jaber-Vazdekis N, García-Expósito L, Machado JD, Zárate R, Ravelo AG, Estévez-Braun A, Valenzuela-Fernández A (2009) The lupane-type triterpene 30-oxo-calenduladiol is a CCR5 antagonist with anti-HIV-1 and anti-chemotactic activities. J Biol Chem 284:16609–16620. CrossRef Medline

Biervert C, Schroeder BC, Kubisch C, Berkovic SF, Propping P, Jentsch TJ, Steinlein OK (1998) A potassium channel mutation in neonatal human epilepsy. Science 279:403–406. CrossRef Medline

Brown DA, Adams PR (1980) Muscarinic suppression of a novel voltage-sensitive K^+ current in a vertebrate neurone. Nature 283:673–676. CrossRef Medline

Brunet A, Park J, Tran H, Hu LS, Hemmings BA, Greenberg ME (2001) Protein kinase SGK mediates survival signals by phosphorylating the forkhead transcription factor FKHRL1 (FOXO3a). Mol Cell Biol 21:952–965. CrossRef Medline

Buckmaster PS (2004) Laboratory animal models of temporal lobe epilepsy. Comp Med 54:473–485. Medline

Cadaveira-Mosquera A, Ribeiro SJ, Reboreda A, Pérez M, Lamas JA (2011) Activation of TREK currents by the neuroprotective agent riluzole in mouse sympathetic neurons. J Neurosci 31:1375–1385. CrossRef Medline

Charlier C, Singh NA, Ryan SG, Lewis TB, Reus BE, Leach RJ, Leppert M (1998) A pore mutation in a novel KQT-like potassium channel gene in an idiopathic epilepsy family. Nat Genet 18:53–55. CrossRef Medline

Chen X, Zhang X, Jia C, Xu J, Gao H, Zhang G, Du X, Zhang H (2011) Membrane depolarization increases membrane PtdIns(4,5)P2 levels through mechanisms involving PKC βII and PI4 kinase. J Biol Chem 286:39760–39767. CrossRef Medline

Debonneville C, Flores SY, Kamynina E, Plant PJ, Tauxe C, Thomas MA, Münster C, Chraïbi A, Pratt JH, Horisberger JD, Pearce D, Loffing J, Staub O (2001) Phosphorylation of Nedd4-2 by Sgk1 regulates epithelial Na(+) channel cell surface expression. EMBO J 20:7052–7059. CrossRef Medline

Delmas P, Brown DA (2005) Pathways modulating neural KCNQ/M (Kv7) potassium channels. Nat Rev Neurosci 6:850–862. CrossRef Medline

Ekberg J, Schuetz F, Boase NA, Conroy SJ, Manning J, Kumar S, Poronnik P, Adams DJ (2007) Regulation of the voltage-gated K(+) channels KCNQ2/3 and KCNQ3/5 by ubiquitination. Novel role for Nedd4-2. J Biol Chem 282:12135–12142. CrossRef Medline

Etxeberria A, Santana-Castro I, Regalado MP, Aivar P, Villarroel A (2004) Three mechanisms underlie KCNQ2/3 heteromeric potassium M-channel potentiation. J Neurosci 24:9146–9152. CrossRef Medline

Falkenburger BH, Jensen JB, Hille B (2010a) Kinetics of PIP2 metabolism and KCNQ2/3 channel regulation studied with a voltage-sensitive phosphatase in living cells. J Gen Physiol 135:99–114. CrossRef Medline

Falkenburger BH, Jensen JB, Dickson EJ, Suh BC, Hille B (2010b) Phosphoinositides: lipid regulators of membrane proteins. J Physiol 588:3179–3185. CrossRef Medline

Gamper N, Stockand JD, Shapiro MS (2003) Subunit-specific modulation of KCNQ potassium channels by Src tyrosine kinase. J Neurosci 23:84–95. Medline

Gamper N, Li Y, Shapiro MS (2005) Structural requirements for differential

sensitivity of KCNQ K^+ channels to modulation by Ca^{2+}/calmodulin. Mol Biol Cell 16:3538–3551. CrossRef Medline

Gehrmann T, Heilmeyer LM Jr (1998) Phosphatidylinositol 4-kinases. Eur J Biochem 253:357–370. CrossRef Medline

Giráldez T, de la Peña P, Gómez-Varela D, Barros F (2002) Correlation between electrical activity and intracellular Ca^{2+} oscillations in GH3 rat anterior pituitary cells. Cell Calcium 31:65–78. CrossRef Medline

Gómez-Posada JC, Etxeberría A, Roura-Ferrer M, Areso P, Masin M, Murrell-Lagnado RD, Villarroel A (2010) A pore residue of the KCNQ3 potassium M-channel subunit controls surface expression. J Neurosci 30:9316–9323. CrossRef Medline

Gómez-Posada JC, Aivar P, Alberdi A, Alaimo A, Etxeberría A, Fernández-Orth J, Zamalloa T, Roura-Ferrer M, Villace P, Areso P, Casis O, Villarroel A (2011) Kv7 channels can function without constitutive calmodulin tethering. PLoS One 6:e25508. CrossRef Medline

Gutman GA, Chandy KG, Adelman JP, Aiyar J, Bayliss DA, Clapham DE, Covarriubias M, Desir GV, Furuichi K, Ganetzky B, Garcia ML, Grissmer S, Jan LY, Karschin A, Kim D, Kuperschmidt S, Kurachi Y, Lazdunski M, Lesage F, Lester HA, et al. (2003) International Union of Pharmacology. XLI. Compendium of voltage-gated ion channels: potassium channels. Pharmacol Rev 55:583–586. CrossRef Medline

Hadley JK, Passmore GM, Tatulian L, Al-Qatari M, Ye F, Wickenden AD, Brown DA (2003) Stoichiometry of expressed KCNQ2/KCNQ3 potassium channels and subunit composition of native ganglionic M channels deduced from block by tetraethylammonium. J Neurosci 23:5012–5019. Medline

Henke G, Maier G, Wallisch S, Boehmer C, Lang F (2004) Regulation of the voltage gated K^+ channel Kv1.3 by the ubiquitin ligase Nedd4-2 and the serum and glucocorticoid inducible kinase SGK1. J Cell Physiol 199:194–199. CrossRef Medline

Hernandez CC, Zaika O, Tolstykh GP, Shapiro MS (2008) Regulation of neural KCNQ channels: signalling pathways, structural motifs and functional implications. J Physiol 586:1811–1821. CrossRef Medline

Jentsch TJ (2000) Neuronal KCNQ potassium channels: physiology and role in disease. Nat Rev Neurosci 1:21–30. CrossRef Medline

Kamynina E, Debonneville C, Bens M, Vandewalle A, Staub O (2001) A novel mouse Nedd4 protein suppresses the activity of the epithelial Na+ channel. FASEB J 15:204–214. CrossRef Medline

Kobayashi T, Cohen P (1999) Activation of serum- and glucocorticoid-regulated protein kinase by agonists that activate phosphatidylinositide 3-kinase is mediated by 3-phosphoinositide-dependent protein kinase-1 (PDK1) and PDK2. Biochem J 339:319–328. Medline

Kosenko A, Kang S, Smith IM, Greene DL, Langeberg LK, Scott JD, Hoshi N (2012) Coordinated signal integration at the M-type potassium channel upon muscarinic stimulation. EMBO J 31:3147–3156. CrossRef Medline

Lalioti M, Heath J (2001) A new method for generating point mutations in bacterial artificial chromosomes by homologous recombination in *Escherichia coli*. Nucleic Acids Res 29:E14. CrossRef Medline

Lamas JA (1998) A hyperpolarization-activated cation current (Ih) contributes to resting membrane potential in rat superior cervical sympathetic neurones. Pflugers Arch 436:429–435. CrossRef Medline

Lamas JA, Reboreda A, Codesido V (2002) Ionic basis of the resting membrane potential in cultured rat sympathetic neurons. Neuroreport 13:585–591. CrossRef Medline

Lamas JA, Romero M, Reboreda A, Sánchez E, Ribeiro SJ (2009) A riluzole- and valproate-sensitive persistent sodium current contributes to the resting membrane potential and increases the excitability of sympathetic neurones. Pflugers Arch 458:589–599. CrossRef Medline

Li Y, Langlais P, Gamper N, Liu F, Shapiro MS (2004) Dual phosphorylations underlie modulation of unitary KCNQ K(+) channels by Src tyrosine kinase. J Biol Chem 279:45399–45407. CrossRef Medline

Li Y, Gamper N, Hilgemann DW, Shapiro MS (2005) Regulation of Kv7 (KCNQ) K+ channel open probability by phosphatidylinositol 4,5-bisphosphate. J Neurosci 25:9825–9835. CrossRef Medline

Loew LM (2007) Where does all the PIP2 come from? J Physiol 582:945–951. CrossRef Medline

Lothman EW, Collins RC (1981) Kainic acid induced limbic seizures: metabolic, behavioral, electroencephalographic and neuropathological correlates. Brain Res 218:299–318. CrossRef Medline

Magistretti J, Mantegazza M, de Curtis M, Wanke E (1998) Modalities of distortion of physiological voltage signals by patch-clamp amplifiers: a modeling study. Biophys J 74:831–842. CrossRef Medline

Marrion NV (1997) Control of M-current. Annu Rev Physiol 59:483–504. CrossRef Medline

Marrion NV, Smart TG, Marsh SJ, Brown DA (1989) Muscarinic suppression of the M-current in the rat sympathetic ganglion is mediated by receptors of the M1-subtype. Br J Pharmacol 98:557–573. CrossRef Medline

McCord MC, Lorenzana A, Bloom CS, Chancer ZO, Schauwecker PE (2008) Effect of age on kainate-induced seizure severity and cell death. Neuroscience 154:1143–1153. CrossRef Medline

Nakajo K, Kubo Y (2005) Protein kinase C shifts the voltage dependence of KCNQ/M channels expressed in *Xenopus* oocytes. J Physiol 569:59–74. CrossRef Medline

Neher E (1992) Correction for liquid junction potentials in patch clamp experiments. Methods Enzymol 207:123–131. CrossRef Medline

Palmada M, Dieter M, Boehmer C, Waldegger S, Lang F (2004) Serum and glucocorticoid inducible kinases functionally regulate ClC-2 channels. Biochem Biophys Res Commun 321:1001–1006. CrossRef Medline

Poët M, Kornak U, Schweizer M, Zdebik AA, Scheel O, Hoelter S, Wurst W, Schmitt A, Fuhrmann JC, Planells-Cases R, Mole SE, Hübner CA, Jentsch TJ (2006) Lysosomal storage disease upon disruption of the neuronal chloride transport protein ClC-6. Proc Natl Acad Sci U S A 103:13854–13859. CrossRef Medline

Racine RJ (1972) Modification of seizure activity by electrical stimulation. II. Motor seizure. Electroencephalogr Clin Neurophysiol 32:281–294. CrossRef Medline

Rae J, Cooper K, Gates P, Watsky M (1991) Low access resistance perforated patch recordings using amphotericin B. J Neurosci Methods 37:15–26. CrossRef Medline

Raikwar NS, Snyder PM, Thomas CP (2008) An evolutionarily conserved N-terminal Sgk1 variant with enhanced stability and improved function. Am J Physiol Renal Physiol 295:F1440–F1448. CrossRef Medline

Romero M, Reboreda A, Sánchez E, Lamas JA (2004) Newly developed blockers of the M-current do not reduce spike frequency adaptation in cultured mouse sympathetic neurons. Eur J Neurosci 19:2693–2702. CrossRef Medline

Schmittgen TD, Livak KJ (2008) Analyzing real-time PCR data by the comparative C(T) method. Nat Protoc 3:1101–1108. CrossRef Medline

Schroeder BC, Kubisch C, Stein V, Jentsch TJ (1998) Moderate loss of function of cyclic-AMP-modulated KCNQ2/KCNQ3 K+ channels causes epilepsy. Nature 396:687–690. CrossRef Medline

Schuetz F, Kumar S, Poronnik P, Adams DJ (2008) Regulation of the voltage-gated K(+) channels KCNQ2/3 and KCNQ3/5 by serum- and glucocorticoid-regulated kinase-1. Am J Physiol Cell Physiol 295:C73–C80. CrossRef Medline

Schwake M, Pusch M, Kharkovets T, Jentsch TJ (2000) Surface expression and single channel properties of KCNQ2/KCNQ3, M-type K+ channels involved in epilepsy. J Biol Chem 275:13343–13348. CrossRef Medline

Schwake M, Jentsch TJ, Friedrich T (2003) A carboxy-terminal domain determines the subunit specificity of KCNQ K+ channel assembly. EMBO Rep 4:76–81. CrossRef Medline

Schwake M, Athanasiadu D, Beimgraben C, Blanz J, Beck C, Jentsch TJ, Saftig P, Friedrich T (2006) Structural determinants of M-type KCNQ (Kv7) K+ channel assembly. J Neurosci 26:3757–3766. CrossRef Medline

Schwarz JR, Glassmeier G, Cooper EC, Kao TC, Nodera H, Tabuena D, Kaji R, Bostock H (2006) KCNQ channels mediate IKs, a slow K+ current regulating excitability in the rat node of Ranvier. J Physiol 573:17–34. CrossRef Medline

Shapiro MS, Roche JP, Kaftan EJ, Cruzblanca H, Mackie K, Hille B (2000) Reconstitution of muscarinic modulation of the KCNQ2/KCNQ3 K^+ channels that underlie the neuronal M current. J Neurosci 20:1710–1721. Medline

Singh NA, Charlier C, Stauffer D, DuPont BR, Leach RJ, Melis R, Ronen GM, Bjerre I, Quattlebaum T, Murphy JV, McHarg ML, Gagnon D, Rosales TO, Peiffer A, Anderson VE, Leppert M (1998) A novel potassium channel gene, KCNQ2, is mutated in an inherited epilepsy of newborns. Nat Genet 18:25–29. CrossRef Medline

Snyder PM, Olson DR, Thomas BC (2002) Serum and glucocorticoid-regulated kinase modulates Nedd4-2-mediated inhibition of the epithelial Na^+ channel. J Biol Chem 277:5–8. CrossRef Medline

Staub O, Dho S, Henry P, Correa J, Ishikawa T, McGlade J, Rotin D (1996) WW domains of Nedd4 bind to the proline-rich PY motifs in the epithe-

lial Na+ channel deleted in Liddle's syndrome. EMBO J 15:2371–2380. Medline

Suh BC, Hille B (2002) Recovery from muscarinic modulation of M current channels requires phosphatidylinositol 4,5-bisphosphate synthesis. Neuron 35:507–520. CrossRef Medline

Tinel N, Diochot S, Lauritzen I, Barhanin J, Lazdunski M, Borsotto M (2000) M-type KCNQ2-KCNQ3 potassium channels are modulated by the KCNE2 subunit. FEBS Lett 480:137–141. CrossRef Medline

Tzingounis AV, Nicoll RA (2008) Contribution of KCNQ2 and KCNQ3 to the medium and slow afterhyperpolarization currents. Proc Natl Acad Sci U S A 105:19974–19979. CrossRef Medline

Wang HS, Pan Z, Shi W, Brown BS, Wymore RS, Cohen IS, Dixon JE, McKinnon D (1998) KCNQ2 and KCNQ3 potassium channel subunits: molecular correlates of the M-channel. Science 282:1890–1893. CrossRef Medline

Wesch D, Miranda P, Afonso-Oramas D, Althaus M, Castro-Hernández J, Dominguez J, Morty RE, Clauss W, González-Hernández T, Alvarez de la Rosa D, Giraldez T (2010) The neuronal-specific SGK1.1 kinase regulates {delta}-epithelial Na+ channel independently of PY motifs and couples it to phospholipase C signaling. Am J Physiol Cell Physiol 299:C779–C790. CrossRef Medline

Wesch D, Althaus M, Miranda P, Cruz-Muros I, Fronius M, González-Hernández T, Clauss WG, Alvarez de la Rosa D, Giraldez T (2012) Differential N termini in epithelial Na+ channel δ-subunit isoforms modulate channel trafficking to the membrane. Am J Physiol Cell Physiol 302:C868–C879. CrossRef Medline

Winks JS, Hughes S, Filippov AK, Tatulian L, Abogadie FC, Brown DA, Marsh SJ (2005) Relationship between membrane phosphatidylinositol-4,5-bisphosphate and receptor-mediated inhibition of native neuronal M channels. J Neurosci 25:3400–3413. CrossRef Medline

Zaika O, Lara LS, Gamper N, Hilgemann DW, Jaffe DB, Shapiro MS (2006) Angiotensin II regulates neuronal excitability via phosphatidylinositol 4,5-bisphosphate-dependent modulation of Kv7 (M-type) K+ channels. J Physiol 575:49–67. CrossRef Medline

Zaika O, Hernandez CC, Bal M, Tolstykh GP, Shapiro MS (2008) Determinants within the turret and pore-loop domains of KCNQ3 K+ channels governing functional activity. Biophys J 95:5121–5137. CrossRef Medline

Zhang H, Craciun LC, Mirshahi T, Rohács T, Lopes CM, Jin T, Logothetis DE (2003) PIP(2) activates KCNQ channels, and its hydrolysis underlies receptor-mediated inhibition of M currents. Neuron 37:963–975. CrossRef Medline

Zhang X, Chen X, Jia C, Geng X, Du X, Zhang H (2010) Depolarization increases phosphatidylinositol (PI) 4,5-bisphosphate level and KCNQ currents through PI 4-kinase mechanisms. J Biol Chem 285:9402–9409. CrossRef Medline